IMPROVING MEDICAL IMAGE PIXEL QUALITY USING MICQ UNSUPERVISED MACHINE LEARNING TECHNIQUE

Syed Thouheed Ahmed[1*], Sreedhar Kumar S[2], Nirmala S Guptha[3], Lavanya N L[4] ,Syed Muzamil Basha[5], Afifa Salsabil Fathima[6]

[1]School of Computing and Information Technology, REVA University, Bengaluru, India

[2]Department of Computer Science and Engineering, Dr. T. Thimmaiah Institute of Technology, KGF, India

[3]Sri Venkateshwara College of Engineering, Visveswaraya Technological University, Bengaluru, India

[4]Department of Computer Science and Engineering, Sapthagiri College of Engineering, Bengaluru, India

[5]School of Computer Science and Engineering, REVA University, Bengaluru, India

[6]School of Engineering, Presidency University, Bengaluru, India

Email: syed.edu.in@gmail.com[1*] (corresponding author)

DOI: https://doi.org/10.22452/mjcs.sp2022no2.5

ABSTRACT

*Biomedical image processing and decision making is a growing research demand under global pandemic situation. The quality of medical images plays a vital role in streamlining remote diagnosis and processing via telemedicine platform, in providing unambiguous results and decision supports. This paper presents an improved Medical Image Content Quality (MICQ) technique and it aims to enrich the Magnetic Resonance (MR) image content or pixels based on semi supervised clustering technique for the process of deeper analysis and investigation to identify the normal and abnormal portions. The proposed (IMICQ) system is containing three stages namely pre-processing, clustering and validation respectively. In the pre-processing stage, the MICQ divides the MR image into finite number of non-overlapping blocks or vectors with size (2*2). Next stage, the proposed MICQ system iteratively partitions the MR image dataset or vector set into optimum number of highly relative dissimilar clusters based on K-Means clustering technique. In the last stage, the proposed system measures the quality of clustering result which obtained in the previous stage based on Effective Cluster Validation Measure (ECVM). Experimental results show that the MICQ is better suitable to improve MR image content quality for telemedicine platform and to predict the normal and abnormal portions over the image with higher accuracy ratio.*

Keywords: Feature Extraction, K-Means, Magnetic Resonance Imaging, Validation, Unsupervised concept

1.0 INTRODUCTION

Medical image processing based decision making is extensively used in evaluating and validating remote consultation and diagnosis due to global pandemic situation. The Global pandemic situation has caused a major medical ecosystem demand with respect to the service. To address COVID-19 based demand many prominent techniques and research approaches are proposed such as detection of COVID-19 from MRI and X-Ray medical images. These approaches are focused on deploying information and extracting the decision support, but fail to address the importance of retrieving image sample-set quality. The intermediating channel of communication applies third party optimization algorithms resulting in image quality tampering and improper representation of data in processing unit. These images produce a false-positive result on real-time trails. Thus, a dedicated framework or technique is required to assure the upliftment of image (medical) quality restoration and enhancement while transmitting over third party real-time channels such as telemedicine platform.

The Magnetic Resonance Imaging (MRI) gives better visual of internal structures of human body. It is widely accepted image processing technique for disease detection, diagnosis and treatment monitoring respectively. With technological advancement it has come to a certain respect where it can detect any diseases in a very short time with full accuracy. Image Segmentation is commonly used technique for partitioning an image into multiple regions. It is considered as an important component in digital image processing. Unsupervised segmentation is beneficial as it does not require training data to segment images and therefore is helpful in the absence of a

manually-labeled dataset. It is important to explore new methodologies as unsupervised segmentation is effective for some but not all classes of images. This facilitates expansion of suitable options for unsupervised segmentation of various classes of medical images. Segmenting medical images, identifying the pixels of organs or tumors from MRI images, remains one of the challenging tasks in analysis of medical images. The proposed technique (MICQ) is based on the pixel segmentation ratio validation and attribute alignment to assure the quality of image is improvised compared to the existing techniques.

2.0 RELATED WORK

Many imaging techniques have been used for image segmentation, like thresholding, region growing, statistical models, active control models and clustering. The distribution of intensities is very complex in medical images, and therefore, identifying a threshold is difficult and thresholding methods fail. Mostly, thresholding method in [1] is combined with other methods. The region growing method is an extension of thresholding. This method requires seed for each region and has the disadvantage of thresholding in finding suitable threshold for homogeneity.

A technique that used Gaussian distribution to estimate the image threshold. [2] Gaussian distribution assumes that the histogram of the image has symmetric distribution. For a non-symmetric histogram, a more generic distribution, i.e. a Gamma distribution, must be used. The proposed method tested on MRI brain images showed good segmentation. An approach of Inherent Image Pixel Classification (IIPC) using an improved agglomerative clustering scheme. It automatically identifies distinct number of different patterns over the medical gray scale images for deeper investigation and analysis. This approach includes Clustering and Validation stages. Performance improvement and complexity reduction in the segmentation process on medical images is achieved using an [3] approach that investigated Berkeley Wavelet Transformation (BWT) based brain tumor segmentation. The accuracy and quality rate of the Support Vector Machine (SVM) based [4] classifier is improved by extracting relevant features from each segmented tissue.

The outcome of proposed technique has been validated in terms of performance and quality analysis on MRI brain images.The automatic segmentation and detection of brain tumor which is a complicated issue and techniques are limited for detection of tumor in multimodal brain MRI. [6] analyses the performance of segmentation using improved Fuzzy C-Means clustering (FCMC) method and marker-controlled watershed method to carry out accurate brain tumor detection and enhance the segmentation results. The main problem associated with the fuzzy C-Means clustering is the selection of initial centroid, [8] Modified version of Fuzzy C-Means technique and Watershed algorithm was used. Three operational noise removal, skull stripping and contrast enhancement was performed before segmentation in pre-processing stage. [17]

Detection of brain tumour from MR images of the brain using Clustering for segmentation [9][13]. K-means Clustering and Fuzzy C Means are used to locate and extract tumour [13]. Another technique is use of Morphological operators along with basic image processing techniques to separate the tumour cells from normal cells. [14] Hybrid methodology of combining Support Vector Machine and Fuzzy C-Means is used to cluster the image for classification. Another technique is histogram-based segmentation [11][12]. The histogram gives an outline of the intensities in an image, but fails to provide information regarding spatial relationships between pixels. Image Enhancement is used to enhance contrast ratio, brightness, remove noise from image and makes identification easier. The drawback of this technique is that the process used to identify the significant variations in the image may be quite complicated. [16] A different approach that splits the image feature vector set that is pre-trained into unique clusters was proposed. In the preprocessing stage, feature vector set of the image is trained using the feature extraction and selection. The size of the image feature vector set is reduced. [20] In Classification stage, clusters are obtained from the trained image feature vector through the k-Means technique.

3.0 PROPOSED APPROACH

The section provides the details of proposed (IMICQ) system and its stages including pre-processing, clustering and validation respectively. In the pre-processing stage, the IMICQ splits the MR image in to finite number of non-overlapping blocks or vectors. Clustering stage, the proposed system identifies limited number of different clusters over the MR image vector set based on K-Means technique and similarity measure. In the last stage, the IMICQ measures the intra similarity and intra dissimilarity over the clustering result with K clusters based on (ECVM). The stages involved in the proposed IMICQ as illustrated in the Figure 1.

3.1 Pre-processing Stage

This stage, the proposed IMIQC system splits the digital representation of MR image (I) with size (H*W) into finite number of non-overlapping blocks or vectors (X) with size of (2*2) and is defined as $X = x_i$, $x_i = x_{ij}$, for $i = 0,1,2,..,n$ where (I)denotes the input MR image with (H*W) pixels, H represents the number of rows in the MR image digital representation (I), W describes the number of Column over the digital representation of MR image (I), X represents the MR image vector set with n vectors with size of d elements, x_i is the ith vector in the vector set X, x_{ij} denotes the jth element in the ith vector which belongs into the MR image vector set (X), n describes the number of vectors in the MR image vector set (X) and is defined in the equation as (1).

$$n = \left\{ \left\{ \frac{H \times W}{d} \right\}, H, W \in I, d = 2 \times 2 \right\} \tag{1}$$

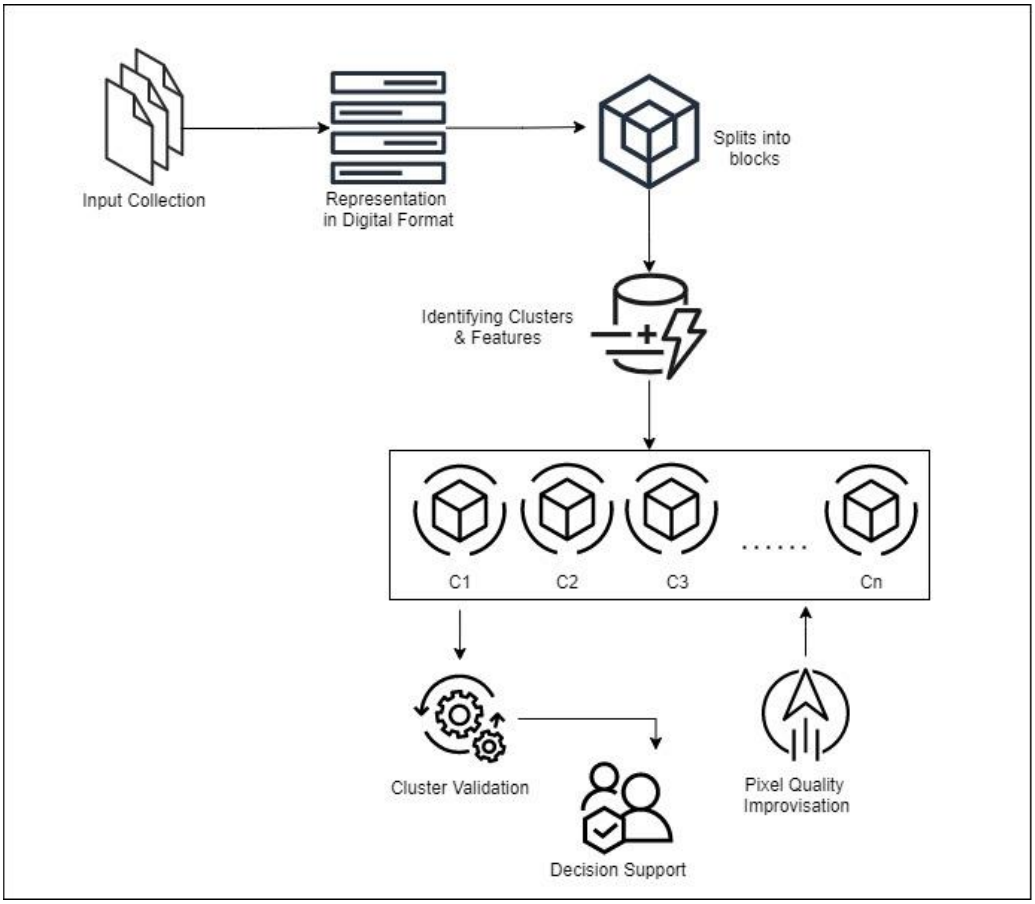

Fig. 1: Framework for Proposed Method

3.2 Clustering Stage

In this clustering stage, the proposed IMICQ system iteratively splits the input MR image vector set (X) into K dissimilar clusters based on K-Means technique and it represents the each individual cluster into separate image for analysis process. The clustering stage consists of four steps, in the first step, it select the k centroid vectors $\bar{V} = \bar{v}_r$, for $r = 0,1,..k$, $\bar{V} \subseteq X$, $\forall \bar{v}_r \in X$ over the actual MR image vector set $X = x_i$, $x_i = x_{ij}$, for $i = 0,1,2,..,n$, $j = 0,1,..d$ based on predetermined knowledge, where k denotes the number of clusters or centroid values, $\bar{V}$ is the centroid vector set with k vectors, $\bar{v}_j$ denotes the rth centroid vector with d pixels which belongs into the centroid vector set $\bar{V}$, X is the medical image vector set with n vectors and d represents the size of the vector. [18]

In the second step, it measures the dissimilarity $D(X,\bar{V})$ between the medical image vector set $X = x_i$ for $i = 0,1,2,..,n$ and centroid vector set $\bar{V} = \bar{v}_r$ for $r = 0,1,..k$ based on Euclidean distance and is defined in the Equation (2).

$$D(X,\bar{V}) = \left\{ \left\{ \underset{r=0,i=0.j=0}{\overset{k-1,n-1,d-1}{d(x_{ij},\bar{v}_{rj})}} \right\} \quad \forall \bar{v}_r \in \bar{V}, \bar{V} \subseteq X, \forall x_i \in X, \forall x_{ij} \in x_i \right\} \tag{2}$$

Where, $d(x_{ij},\bar{v}_{rj})$ denotes the Euclidean distance between jth pixels of rth centroid vector and ith input medical image vector and is defined in the equation (3)

$$d(x_{ij},\bar{v}_{rj}) = \left\{ \left[\sum_{j=0}^{d-0} (x_{ij} - \bar{v}_{rj})^2 \right]^{1/2} \right\} \tag{3}$$

Next step, it place the each individual ith vector x_i in the X into their closest centroid vector $\bar{v}_r$ of its respective cluster c_r in the cluster set $C = c_r$ for $r = 0,1,..,k$ based on the highest similarity and is defined in the Equation (4) as

$$c_r = Min\left\{ \left\{ \underset{r-0,i=0}{\overset{k-1,n-1}{d(x_i,\bar{v}_r)}} \right\}, \forall c_r \subseteq X \right\} \tag{4}$$

Where, C denotes the predetermined cluster set with k clusters, c_r represents the rth cluster in the cluster set C and in the last step, it updates the rth centroid vector value $\bar{V} = \bar{v}_r$ of each individual cluster $C = c_r$ based on vectors in their respective rth cluster and is defined in the Equation (5) as

$$\bar{v}_r = \left\{ \left\{ \frac{1}{|c_r|} \times \sum_{e=1}^{|c_r|} c_{re} \right\}, \quad \forall c_{re} \in c_r \right\} \tag{5}$$

Where, $|c_r|$ denotes the number of similar MR image vectors and c_{re} represents the eth vector in the rth cluster which belongs into cluster set C. The process of updating center is iterated until a situation where centers do not change anymore or criterion function becomes lesser and the clustering stage algorithm is described in the below sub section.

3.2.1 K-Means Algorithm

Algorithm: K Means

Input: MR Image Vector Set $X = x_i$ with n vectors, Centroid Vector Set $\bar{V} = \bar{v}_r$ with k Vectors
Output: Produced k Distinct Clusters $C = \{c_1, c_2, ..c_k\}$
Begin

1. Randomly select k number of centroid vectors over the MR image vector set X with n vectors and assigned into $\bar{V} = \bar{v}_r$ for $r = 1,2,3..,k$
2. Iteratively computes the Euclidean distance between centroid vector set $\bar{V} = \bar{v}_r$ and MR image vector $X = x_i$ using Equations (2) and (3)
3. Place the each individual vector in the MR image vector set $X = x_i$ into its closest cluster centroid cluster based on higher similarity using Equation (4)

4. Update the each individual rth cluster centroid $(\bar{v}_r)$ based on elements or vectors of the rth cluster by Equation (5)
5. Repeat the steps from 2 to 4 until the present iteration cluster centroid is similar to previous iteration.

End

3.3 Cluster Validation Stage

This stage, the proposed (IMICQ) system measures the quality of the clusters through the process of estimating the intra similarity and intra dissimilarity among the vectors within the each individual cluster in the cluster set $C = c_r$ for $r = 0,1,..,k$ based on Effective Cluster Validation Method [21]. The ECVM consists of two measures namely intra cluster similarity and intra cluster divergence respectively.

3.3.1 Intra Cluster Similarity

It computes the similarity among the vectors in the each individual cluster which belongs into the cluster set $C = c_r$ for $r = 0,1,..,k$. This measure consists of three steps, in the first step, it computes the cluster centroid $\bar{C} = \bar{c}_r$ for $r = 0,1,..,k$ of each individual cluster in the cluster set $C = c_r$ and is defined in the equation (6) as.

$$\bar{c}_r = \left\{ \left\{ \frac{1}{|c_r|} \times \sum_{e=1}^{|c_r|} c_{re} \right\}, \quad \forall c_{re} \in c_r \right\} \tag{6}$$

Where, $|c_r|$ denotes the number of similar MR image vectors in the rth cluster which belongs into cluster set and c_{re} represents the eth vector with d pixels in the rth cluster c_r which belongs into cluster set C. In the next step, it calculates the intra similarity $S = s_r$ for $r = 0,1,..,k$ among the vectors within the each individual cluster $C = c_r$ for $r = 0,1,..,k$ based on cluster centroids $\bar{C} = \bar{c}_r$ for $r = 0,1,..,k$, where s_r denotes the measure of intra similarity among the vectors in the rth cluster c_r in the cluster set C and S represents the intra similarity set with similarity of k clusters and is defined in the Equation (7) as

$$s_r = \left\{ \frac{\sum_{e=1}^{|c_r|} \sum_{j}^{d-1} \left| c_{rej} - \bar{c}_{rj} \right|}{|c_r|} \times 100 \;\middle|\; \forall \bar{c}_{rj} \in \bar{c}_r, \quad \forall c_{re} \in c_r, \quad where \begin{cases} 1 & \left| c_{rej} - \bar{c}_{rj} \right| <= T \\ 0 & \left| c_{rej} - \bar{c}_{rj} \right| > T \end{cases} \right\} \tag{7}$$

where $\bar{c}_r$ represents the rth cluster centroid of the rth cluster c_r which belongs into cluster set C and T is the threshold value which uses to limit the similarity and dissimilarity among the cluster vector $c_r = c_{re}$ and centroid of the each individual cluster $\bar{C} = \bar{c}_r$. Finally, it computes the overall intra-cluster similarity $IS(C)$ over the cluster set $C = c_r$ for $r = 0,1,..,k$ based on intra similarity of each individual cluster $S = s_r$ for $r = 0,1,..,k$ and is defined in the equation (8),

$$IS(C) = \left\{ \frac{\sum_{r=1}^{k} s_r}{k} \right\} \tag{8}$$

3.3.2 Intra-Cluster Dissimilarity

It finds the intra-cluster dissimilarity or divergence within each individual cluster over the clustering result. It follows two steps, in the first step, it finds the divergence $D = d_r$ for $r = 0,1,..,k$ of each individual cluster in the

cluster $C = c_r$ based on cluster centroid $\overline{C} = \overline{c}_r$ where, d_r denotes the dissimilarity measures over the rth cluster c_r in the cluster set $C = c_r$ for $r = 0,1,..,k$ and it is given in the equation (9),

$$d_r = \left\{ \frac{\sum_{e=1}^{|c_r|} \sum_{j}^{d-1} \left| c_{rej} - \overline{c}_{rj} \right|}{|c_r|} \times 100 \;\middle|\; \forall \overline{c}_{rj} \in \overline{c}_r, \quad \forall c_{re} \in c_r, \quad where \begin{cases} 0 & \left| c_{rej} - \overline{c}_{rj} \right| <= T \\ 1 & \left| c_{rej} - \overline{c}_{rj} \right| > T \end{cases} \right\} \tag{9}$$

Finally, it computes the overall intra-cluster divergence $ID(C)$ over the cluster set $C = c_r$ for $r = 0,1,..,k$ based on intra dissimilarity of each individual cluster $D = d_r$ for $r = 0,1,..,k$ and is defined in the equation (10),

$$ID(C) = \left\{ \frac{\sum_{r=1}^{k} d_r}{k} \right\} \tag{10}$$

Where divergence of the rth cluster is given by d_r in the resulting cluster $C = c_r$ for $r = 0,1,..,k$ and k is the total number of clusters in the resulting cluster C. The experimental results of the proposed technique are discussed in the next section.

Algorithm: Clustering of MRI datasets

Input: Cluster set C containing k Distinct Clusters

Output: Intra-Similarity $IS(C)$ and Intra-Divergence $ID(C)$

Begin

1. Calculates the centroid $\overline{C} = \overline{c}_r$ of each individual cluster over the $C = c_r$ for $r = 0,1,..,k$ using equation (6).
2. Compute the intra similarity $S = s_r$ among the objects in each individual cluster $C = c_r$ based on centroid $\overline{C} = \overline{c}_r$ of the clusters as expressed in equation (6)
3. Evaluate the overall intra similarity $IS(C)$ of cluster set $C = c_r$ using equation (7)
4. Compute the intra dissimilarity $D = d_r$ of each individual cluster over the cluster set $C = c_r$ based on centroid $\overline{C} = \overline{c}_r$ of each individual cluster r = 1, 2,.., k using equation (8).
5. Calculate the overall intra divergence of the result Rc based on IP = IP_i for I = 1, 2,.., k using equation (9) and the result is obtained in $ID(C)$. [19]

   End

4.0 RESULTS AND DISCUSSIONS

The datasets are in alignment with the kaggle (MRI) relevance, the datasets considered are highlighted with primary feature dimensions and parameters. The experimental analysis considers 2823 datasets on MRI with a pertaining validation from The Cancer Image Archive (CIA). The training and testing is processed under 60:40 ratio for improvising the analysis and decision making. Results obtained for the proposed MICQ approach is discussed in this section. For the experiment, Grayscale MR image of size 100*100 as shown in the Figure 2. The quality of image samples in the initial parametric evaluation. The input image is divided into 2500 blocks of 2*2 size. In feature extraction stage, three statistical operators such as mean, standard deviation and variance are applied to each of the block. It results in Image Feature Vector Set. Now, the blocks have only three features. The image feature vector set is given as an input to K-Means technique and three dissimilar clusters C_0, C_1, C_2 are obtained and the clustering results as illustrated in the Figure 3.

Clusters are represented as individual images as shown in Figure 3. It can be clearly noticed that specific portions are extracted and can be used for deep investigations. But these images need further enhancement for accurate analysis. Pixel quality of these clusters is improved in terms of brightness and contrast using arithmetic operations. Improved MRI Image as shown in Figure 4 is obtained after applying arithmetic operation for enhancing contrast/ brightness on all the clusters. The computational matrix of cluster representation of information with reference to originality of the processing file is computed in Table. 1 towards validating the accuracy of processed data, similarity and divergence. The range of variation is retrieved from (0 – 1) to assure the processing grounds for pixel quality improvisation. The proposed MICQ approach has successfully improved the quality of image (input) to the retrieved output as shown in Table. 2. The accuracy of each cluster index of range C_0, C_1, C_2 is optimized with $C_{n\text{-}OPT}$ for internal optimization of processing data's reliability factor computation.

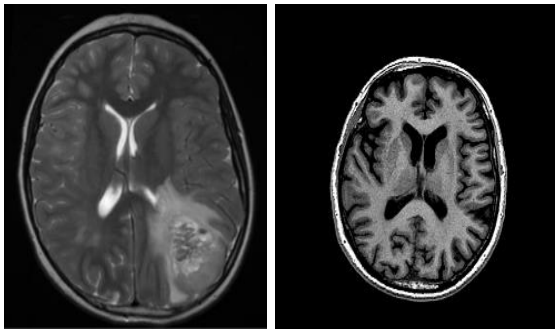

(a) (b)

Fig. 2: Original MRI Image (a) Image 1 (b) Image 2

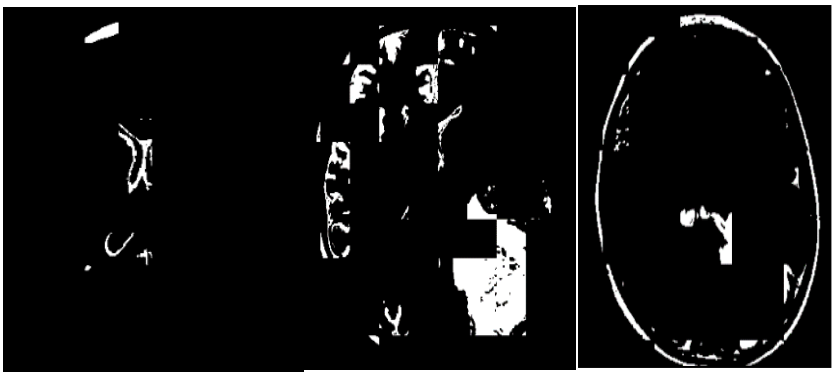

(a)

(b)

Fig. 3: Result of K-Means Algorithm showing distinct clusters as individual images for (a) Image 1 (b) Image 2

The effectiveness of clustering has been validated. The Intra-cluster similarity and Intra-cluster divergence is calculated for each of the clusters. The results are shown in Table 1 for Clusters C_0, C_1, C_2 respectively.

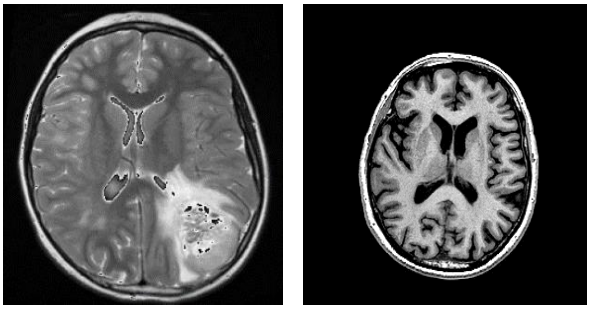

Fig. 4: Improved MRI Image after applying Arithmetic operation on all the Clusters

Table 1: Result of Cluster Validation on Clusters obtained from K-Means Algorithm

Image	Cluster index	Reliability factor (R)	Integrality Validation (I)	Originality range (O_R)	Schematic Value of recurrence	
					Similarity	Divergence
Sample-1: Image (a)						
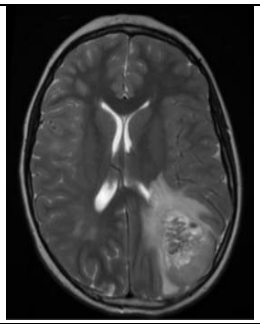	C0	0.453	0.721	0.821	0.835	0.165
	C1	0.478	0.752	0.832	0.921	0.079
	C2	0.481	0.752	0.875	0.965	0.035
	Cn	0.488	0.754	0.879	0.921	0.079
	$(Cn)_{OPT}$	0.493	0.751	0.854	0.896	0.104
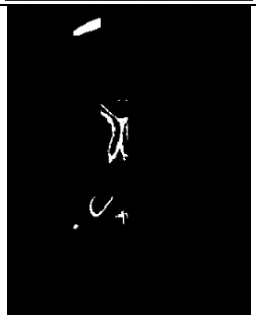	C_0	0.512	0.612	0.862	0.731	0.269
	C_1	0.527	0.675	0.888	0.771	0.229
	C_2	0.553	0.751	0.862	0.821	0.179
	C_n	0.497	0.751	0.854	0.797	0.203
	$(C_n)_{OPT}$	0.511	0.712	0.872	0.761	0.239
	C_0	0.511	0.712	0.872	0.797	0.203
	C_1	0.563	0.782	0.864	0.792	0.208
	C_2	0.527	0.792	0.872	0.811	0.189
	C_n	0.601	0.721	0.864	0.821	0.179
	$(C_n)_{OPT}$	0.528	0.772	0.861	0.821	0.179
	C_0	0.583	0.771	0.932	0.831	0.169
	C_1	0.562	0.792	0.923	0.867	0.133
	C_2	0.583	0.714	0.911	0.823	0.177

	C_n	0.527	0.780	0.917	0.910	0.09
	$(C_n)_{OPT}$	0.528	0.723	0.918	0.899	0.101
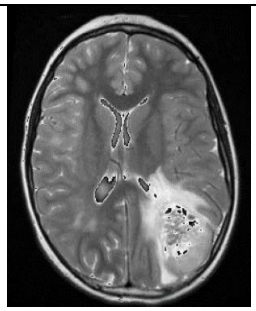	C_0	0.621	0.762	0.912	0.932	0.068
	C_1	0.745	0.780	0.975	0.972	0.028
	C_2	0.712	0.722	0.932	0.892	0.108
	C_n	0.799	0.821	0.947	0.911	0.089
	$(C_n)_{OPT}$	0.743	0.796	0.936	0.937	0.063
Sample-2: Image (b)						
	C_0	0.321	0.732	0.652	0.823	0.177
	C_1	0.321	0.711	0.672	0.752	0.248
	C_2	0.397	0.732	0.661	0.882	0.118
	C_n	0.300	0.712	0.660	0.822	0.178
	$(C_n)_{OPT}$	0.311	0.702	0.661	0.846	0.154
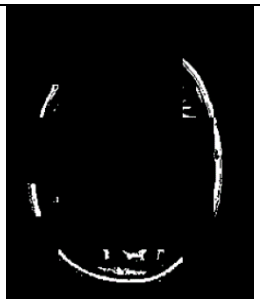	C_0	0.389	0.789	0.721	0.864	0.136
	C_1	0.439	0.792	0.692	0.811	0.189
	C_2	0.492	0.812	0.621	0.823	0.177
	C_n	0.482	0.832	0.661	0.865	0.135
	$(C_n)_{OPT}$	0.521	0.812	0.711	0.838	0.162
	C_0	0.553	0.823	0.724	0.821	0.179
	C_1	0.657	0.811	0.719	0.831	0.169
	C_2	0.611	0.815	0.711	0.861	0.139
	C_n	0.5990	0.891	0.768	0.888	0.112
	$(C_n)_{OPT}$	0.6112	0.861	0.777	0.863	0.137
	C_0	0.723	0.865	0.811	0.921	0.079
	C_1	0.722	0.821	0.821	0.910	0.09
	C_2	0.765	0.711	0.872	0.899	0.101
	C_n	0.745	0.823	0.865	0.917	0.083
	$(C_n)_{OPT}$	0.752	0.854	0.843	0.907	0.093
	C_0	0.771	0.832	0.856	0.923	0.077

	C_1	0.789	0.832	0.882	0.921	0.079
	C_2	0.712	0.898	0.812	0.954	0.046
	C_n	0.782	0.888	0.900	0.954	0.046
	$(C_n)_{OPT}$	0.772	0.854	0.892	0.933	0.067

Table 2: Result Comparative and Validation Analysis

Image	Cluster	Intra-Similarity	Intra-Divergence
1	C_0	93.362389564712	4.186558656128054
	C_1	82.133897670079	28.89228132607802
	C_2	75.676065713643	19.36917615994244
2	C_0	73.019153931073	55.7239938636403
	C_1	83.867912175475	14.4629269848639
	C_2	82.33543724749	15.4843627429900

From the experimental results, it is clearly demonstrated that the proposed approach identifies the clusters that are distinct with high intra-similarity (accuracy) and lower intra-cluster dissimilarity over the medical gray scale images automatically. The output image obtained shows required regions visible with much clarity.

5.0 CONCLUSION

Medical images quality improvisation via pixel enhancement is a research challenge. The quality factors and attribute distribution varies with technological development. In this research article an image segmentation operation is performed on gray-scale MRI images and quality of image is improved on selective regions using unsupervised technique. The proposed approach divides the image feature vector set into clusters with a distinct K-Means clustering technique. Validation ensures better clustering quality under enhanced pixel ratio, the selective Region of Interest (RoI) of medical image are enhanced and over enhancement problem faced in histogram equalization is avoided. The proposed technique has provided a higher order of reliability in improving the medical image quality under communication and storage serves. In near future, the technique can be improved under color image processing techniques.

REFERENCES

[1] A. R. A. Abdulraqeb, W. A. Al-haidri and L. T. Sushkova, "A novel segmentation algorithm for MRI brain tumor images", in *2018 Ural Symposium on Biomedical Engineering, Radioelectronics and Information Technology (USBEREIT)*, 2018, pp. 1-4, doi: 10.1109/USBEREIT.2018.8384535.

[2] W. El Hajj Chehade, R. A. Kader and A. El-Zaart, "Segmentation of MRI images for Brain Cancer Detection", in *International Conference on Information and Communications Technology***,** March 2018, pp. 6-7, doi: 10.1109/ICOIACT.2018.8350721.

[3] N. B. Bahadure and A. K. Ray and H. P. Thethi, "Image Analysis for MRI Based Brain Tumor Detection and Feature Extraction", in *International Journal of Biomedical Imaging*, Vol. 2, No. 5, March 2017, pp.3-6, doi: 10.1155/2017/9749108.

[4] K. D. Kharat, V. J. Pawar and S. R. Pardeshi, "Feature extraction and selection from MRI Images for the Brain Tumor Classification", in *2016 International Conference on Communication and Electronics Systems*, Oct. 2016. pp. 21-22, doi: 10.1109/CESYS.2016.7889969.

[5] K. Bhima and D. A. Jagan, "An Improved Method for Automatic Segmentation and Accurate Detection of Brain Tumor in Multimodal MRI", *International Journal of Image, Graphics and Signal Processing*, Vol. 9, No. 5, May 2017, pp.1-8, doi: 10.5815/ijigsp.2017.05.01.

[6] S. Harish, G. F. A. Ahammed and R. Banu, "An Extensive Research Survey on Brain MRI Enhancement, Segmentation and Classification", in *2017 International Conference on Electrical, Electronics, Communication, Computer, and Optimization Techniques (ICEECCOT)*, Dec. 2017, pp. 1-8, doi: 10.1109/ICEECCOT.2017.8284578.

[7] C. C. Benson, V. Deepa, V. L. Lajish and K. Rajamani, "Brain Tumor Segmentation from MR Brain Images Using Improved Fuzzy C-Means Clustering and Watershed algorithm", in *2016 International Conference on Advances in Computing, Communications and Informatics (ICACCI)*, 2016, pp. 187-192, doi: 10.1109/ICACCI.2016.7732045.

[8] A. Nandi, "Detection of human brain tumour using MRI image segmentation and morphological operators", in *2015 IEEE International Conference on Computer Graphics, Vision and Information Security (CGVIS)*, 2015, pp. 55-60, doi: 10.1109/CGVIS.2015.7449892.

[9] C. Desrosiers, "An unsupervised random walk approach for the segmentation of brain MRI", in *2014 IEEE 11th International Symposium on Biomedical Imaging (ISBI)*, 2014, pp. 337-340, doi: 10.1109/ISBI.2014.6867877.

[10] N. Dhanachandra, K. Manglem and Y. J. Chanu, "Image Segmentation Methods using K-means Clustering Algorithm for Color Image", in *Eleventh International Multi-Conference on Information Processing*, Sept. 2015, pp. 764-771, doi: 10.1016/j.procs.2015.06.090.

[11] H. Kaur and J. Rani, "MRI brain image enhancement using Histogram Equalization techniques," in *2016 International Conference on Wireless Communications, Signal Processing and Networking (WiSPNET)*, 2016, pp. 770-773, doi: 10.1109/WiSPNET.2016.7566237.

[12] B. Srinivas and G. S. Rao, "Unsupervised learning algorithms for MRI brain tumor segmentation," in *2018 Conference on Signal Processing And Communication Engineering Systems (SPACES)*, 2018, pp. 181-184, doi: 10.1109/SPACES.2018.8316341.

[13] Parveen and A. Singh, "Detection of brain tumor in MRI images, using combination of fuzzy c-means and SVM", in *2015 2nd International Conference on Signal Processing and Integrated Networks (SPIN)*, 2015, pp. 98-102, doi: 10.1109/SPIN.2015.7095308.

[14] K. B. Vaishnavee and K. Amshakala, "An automated MRI brain image segmentation and tumor detection using SOM-clustering and Proximal Support Vector Machine classifier", in *2015 IEEE International Conference on Engineering and Technology (ICETECH)*, 2015, pp. 1-6, doi: 10.1109/ICETECH.2015.7275030.

[15] S. T. Ahmed and K. K. Patil, "An investigative study on motifs extracted features on real time big-data signals", in *2016 International Conference on Emerging Technological Trends (ICETT)*, 2016, pp. 1-4, doi: 10.1109/ICETT.2016.7873721.

[16] V. Sathiyamoorthi, A.K. Ilavarasi, K.Murugeswari, S. T. Ahmed, B. A. Devi and M. Kalipindi, "A deep convolutional neural network based computer aided diagnosis system for the prediction of Alzheimer's disease in MRI images", *Measurement*, vol. 171, 2021, pp. 108838, doi: 10.1016/j.measurement.2020.108838.

[17] S. T. Ahmed, M. Sandhya and S.Sankar, "A dynamic MooM dataset processing under TelMED protocol design for QoS improvisation of telemedicine environment", *Journal of medical systems*, Springer, Vol. 43, No. 8, 2019, pp. 1-12, doi: 10.1007/s10916-019-1392-4.

[18] S. S. Kumar, S. T. Ahmed, Q. Xin, S. Sandeep, M. Madheswaran and S. M. Basha,*"Unstructured oncological image cluster identification using improved unsupervised clustering techniques".* Computers, Materials and Continua, Vol. 72, No. 1, 2022, pp. 281-299. doi:10.32604/cmc.2022.023693.

[19] M. Mohammadi, M. Sarmad and N. R. Arghami, "An Extension of the Outlier Map for Visualizing the Classification Results of the Multi-Class Support Vector Machine." *Malaysian Journal of Computer Science*, Vol. 34, No. 3, 2021, pp. 308-323, doi: 10.22452/mjcs.vol34no3.5.